I&EC research
Industrial & Engineering Chemistry Research

Article

Cite This: Ind. Eng. Chem. Res. 2019, 58, 8112−8122

pubs.acs.org/IECR

Assessment of the Thermal Degradation of Sodium Lauroyl Isethionate Using Predictive Isoconversional Kinetics and a Temperature-Resolved Analysis of Evolved Gases

Mohammed I. Jeraal,*[,†] Kevin J. Roberts,[†] Ian McRobbie,[‡] and David Harbottle[†]

[†]School of Chemical and Process Engineering, University of Leeds, Woodhouse Lane, Leeds LS2 9JT, United Kingdom
[‡]Innospec Ltd., Innospec Manufacturing Park, Oil Sites Road, Ellesmere Port CH65 4EY, United Kingdom

Supporting Information

ABSTRACT: Sodium lauroyl isethionate is a popular, milder alternative to traditional soaps and surfactants in personal care formulations. Product performance, efficiency, color, and odor, however, can be compromised by thermal degradation at elevated manufacturing temperatures. Prediction of isothermal degradation rates in both air and N_2 for a range of process conditions are determined using the Friedman isoconversional method. The thermal degradation levels in air are found to be 28 times higher than those in N_2 over 5 h at 240 °C. Manufacturing under inert conditions, with maximum temperatures of 250 °C, is therefore necessary to avoid degradation levels significantly greater than 1 wt %. Using TGA-FTIR, the evolved gases from the degradation of sodium lauroyl isethionate are identified to be water, carbon dioxide, carbon disulfide, sulfur dioxide, as well as alkyl and carbonyl species. The ensuing temperature-dependent analysis can be used to minimize evolution of undesirable or hazardous gases in isethionate manufacturing processes.

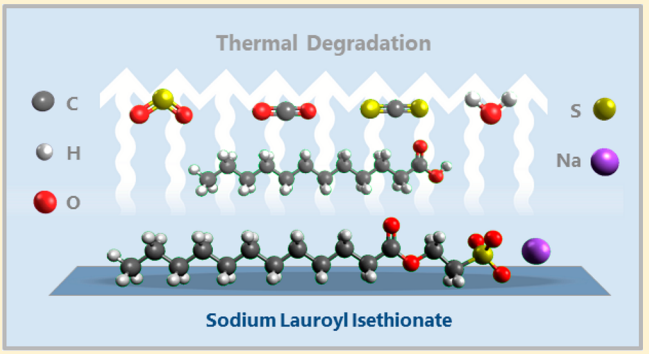

INTRODUCTION

Surfactants are the primary ingredients in most personal care formulations. They are present in shampoos, liquid cleansers, and soap bars to reduce the surface tension of water and aid in the solubilization of lipidic, sebaceous residues on the skin.[1] Due to its mildness, sodium lauroyl isethionate (SLI) is becoming an increasingly popular surfactant in such applications.[2] When compared with traditional counterparts such as alkyl carboxylates and sodium dodecyl sulfate (SDS), studies into SLI have demonstrated reduced irritation,[3] dryness,[4] and adhesion to the stratum corneum[5] in personal care applications. SLI is also comparatively more stable in the presence of hard water by exhibiting no deposit formation or significant loss in lathering abilities in the present of alkali earth metals.[6]

SLI can be synthesized via the esterification of lauric acid with sodium isethionate,[7] as shown in Figure 1. In the cited laboratory synthesis, the materials were reacted at a temperature of 240 °C for 4 h.[7] Patent literature relating to the commercial synthesis of SLI, as well as its homologues, report similar process temperatures of >200 °C and analogous reaction times of 4−6 h.[8−10] In some instances, temperatures as high as 260 °C for prolonged periods have been reported.[11,12] A patent by Login et al. reported that the molten isethionate reaction mixture was prone to thermal degradation at reaction temperatures in excess of 220 °C.[13] In addition to reducing surfactant activity levels and consequent product efficiency, degradation was also reported to significantly harm the appearance and odor of the resulting product.[14] While this work recommended an oxygen-free atmosphere to minimize process-induced degradation, no information pertaining to the quantitative stability of isethionate esters was provided.

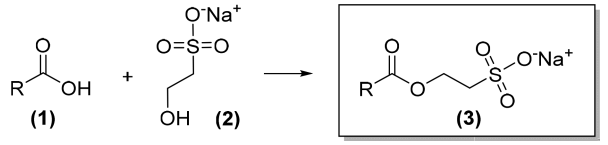

Figure 1. Reaction of lauric acid (**1**) with sodium isethionate (**2**) to form the dodecyl-chained (C12) sodium lauroyl isethionate (SLI) (**3**).[7] In this example, R = $C_{11}H_{25}$. A mixture of chemical homologues of alkyl chain length ranging between C8 and C18 can also be formed from the respective mixture of carboxylic acids. The resulting blend of surfactants is known as sodium cocoyl isethionate (SCI).[7]

While previous research regarding the thermal behavior of isethionates has been limited, there have been studies on the

Received: February 9, 2019
Revised: April 4, 2019
Accepted: April 8, 2019
Published: April 9, 2019

DOI: 10.1021/acs.iecr.9b00797
Ind. Eng. Chem. Res. 2019, 58, 8112−8122

stability and degradation characteristics of other alkyl surfactants, such as SDS. The incipient thermal degradation of SDS was reported as 380 °C,[15] indicating its comparatively higher stability with respect to SLI which thermally degrades at 220 °C.[13] A pyrolysis-gas-chromatography analysis of SDS by Liddicoet et al. identified the degradation products following prolonged exposure to 650 °C under an inert atmosphere.[16] It revealed large quantities of primary alcohol, coupled with traces of dodecyl vinyl chains. While both SDS and SLI consist of analogous lauryl alkyl chains, differences between the chemistry of their respective sulfate and sulfonate groups, coupled with the additional acid−ester group present in SLI might suggest an influence on its resulting material stability and associated evolved gas composition.

For the characterization of thermal degradation processes, kinetic methods are typically applied to quantify the rates at which the underpinning chemical and physical processes occur.[17] These rates allow the evaluation of the corresponding energetic parameters; the correct identification of which permits the prediction of material stability.[18] In contrast to isothermal techniques where degradation is measured at multiple fixed temperatures, nonisothermal (or polythermal) isoconversional methods rely on multiple linear heating experiments to obtain the necessary data for kinetic model development.[19] While isothermal degradation techniques do exhibit some advantages, such as the ease of induction time measurement, their nonisothermal counterparts are becoming the recommended methodology for the kinetic analysis of thermally stimulated processes.[20,21] With isothermal methods, it can be challenging to cover a representative range of temperatures within the measurable degradation zone. Slow degradation rates at lower temperatures can be time-consuming to measure to completion, while isothermal degradation at higher temperatures can be difficult to specifically identify if mass loss occurs while the sample is reaching the desired isotherm.[20] Absolute isothermal analyses can often be difficult to achieve due to this inevitable period of equilibration, particularly when a sample is exposed to elevated temperatures.[19] While differential methods can be applied to help alleviate such discrepancies,[20] nonisothermal analyses can experimentally avoid these shortcomings, while simultaneously allowing the fast acquisition of degradation data across a broad range of temperatures.[17]

In this study, the thermal stability of SLI under the temperatures experienced during representative manufacturing conditions was evaluated. Thermogravimetric analysis (TGA), coupled with isoconversional kinetic modeling, was used to assess the thermal degradation of SLI in N_2 and air environments. Measurement under inert conditions was used to simulate degradation under the representative manufacturing conditions, while the analogous measurements in an oxidative environment were used to determine the influence of air ingress into the process system. Differential and integral isoconversional methods were used to independently quantify critical energetic parameters. These factors were then applied to predict the isothermal degradation of SLI, as a function of temperature, to determine the most suitable process conditions for minimizing degradation. Following the kinetic overview, TGA-FTIR was used to obtain a real-time analysis of the gaseous evolutions resulting from the degradation process.

Isoconversional Kinetic Theory for Thermal Analysis. Thermogravimetric analysis (TGA) and differential scanning calorimetry (DSC) are commonly used to derive the data required to characterize thermal degradation processes using isoconversional kinetic methods.[17] Although TGA will be the focus of the current study, the techniques described can also be applied to data obtained from infrared spectroscopy,[22] mass spectrometry,[23] and rheometry.[24] For the isoconversional kinetic analysis of TGA data, it is common for the experimentally obtained mass losses to be converted to a normalized, dimensionless, temperature-dependent mass loss (α) where $0 < \alpha < 1$.[21] In the context of thermal decomposition kinetics derived via TGA, α is commonly referred to as the "degree of degradation".[20] In this study, eq 1 shows how α was obtained from the initial sample mass before heating (m_{Init}), the final sample mass after heating (m_{Fin}) and the observed sample mass (m_{Curr}) at a given temperature.

$$\alpha = \frac{m_{Init} - m_{Curr}}{m_{Init} - m_{Fin}} \tag{1}$$

Nonisothermal (or polythermal) isoconversional degradation kinetics are fundamentally derived from the Arrhenius equation:

$$k(T) = A \exp\left(-\frac{E_a}{RT}\right) \tag{2}$$

$k(T)$ is the Arrhenius rate constant, A the Arrhenius pre-exponential factor, R the universal gas constant (8.314 J mol^{-1} K^{-1}), E_a the activation energy (J mol^{-1}), and T the absolute temperature in Kelvin. Vyazovkin states that the rate of thermally stimulated processes are dependent on the reaction model $f(\alpha)$ and temperature-dependent rate constant $k(T)$, as shown in eq 3.[21]

$$\left(\frac{d\alpha}{dt}\right) = k(T) f(\alpha) \tag{3}$$

Some forms of the equation include an additional pressure dependent variable $h(P)$. However, in the case of thermal degradation kinetics, this is assumed insignificant and neglected in most cases.[20] Combining eq 2 and 3 yields the general rate equation (eq 4) for the nonisothermal kinetic analysis of thermally stimulated degradation processes.

$$\left(\frac{d\alpha}{dt}\right)_\beta = A \exp\left(-\frac{E_a}{RT}\right) f(\alpha) \tag{4}$$

The rate ($d\alpha/dt$) is a function of heating rate (β), which corresponds to a constant linear heating rate where $\beta = dT/dt$. The reaction model $f(\alpha)$ is dependent on, and consequently indicative of, the thermal degradation mechanism.[25] For conventional isothermal analyses, the type of mechanism can be determined by identifying the relationship between $f(\alpha)$ and α. When fitting experimental data to such models, however, similarity between fits can complicate the identification of a single reaction model.[17] Criado et al. have previously demonstrated how the same predicted TGA curve can be generated from three different reaction models.[26] The model fitting approach can also be overly simplistic with respect to more complex systems, which can exhibit one mechanism at the start of the degradation process, then transition into another at higher degradation temperatures. Equation 3 additionally shows how it can be numerically challenging to mathematically separate and distinguish between $k(T)$ and $f(\alpha)$, thus further increasing the difficulty in obtaining a single reaction model.

DOI: 10.1021/acs.iecr.9b00797
Ind. Eng. Chem. Res. 2019, 58, 8112−8122

Isoconversional kinetics conversely forego the fitting of a reaction model $f(\alpha)$, as well as the calculation of a single pre-exponential factor A. This approach is based on the fundamental assumption that a single form of eq 4 is only applicable to a single degree of degradation (α).[27,28] This temperature dependence on the Arrhenius parameters is proposed on the basis that solid-state thermal decomposition is typically a complex, interdependent multistep chemical process. The multitude of constituent, concurrent physical processes include the diffusion, sorption, and sublimation of different species in multiple phases.[29] Any single activation energy value therefore used to represent a process of corresponding complexity is inherently composed of the individual activation energies related to its constituent physical and chemical processes. Since the relative contributions of these individual processes to the overall degradation rate changes with respect to temperature, any effective activation energy (E_a) determined for the holistic characterization of thermal degradation process is consequently a function of temperature and the degree of degradation (α). Through multirate degradation experiments, values of the temperature-dependent effective activation energy can be obtained following differential or integral treatment of eq 4. Through the parametrization of $f(\alpha)$ and the Arrhenius factor A, predictions of process degradation rates and material lifetimes can be reliably achieved. Compared with traditional isothermal kinetic analyses, nonisothermal isoconversional methods therefore permit the holistic kinetic analysis of complex thermally stimulated processes, without any prior knowledge of the degradation mechanism(s). The concept of variable activation energy, its basis in complex multiple-step processes, as well as its broader application in the characterization of thermal stability, polymerization, crystallization and phase transitions is described in the literature.[30] In order to obtain a more comprehensive analysis of the thermal degradation characteristics of organic materials,[31,32] both isoconversional and model-fitting techniques can be applied in tandem, with research comparing both approaches when studying analogous chemical systems.[33]

Calculation of Activation Energies. Both differential and integral approaches were separately used to calculate the effective activation energy (E_a). The Friedman method is a common differential method for the isoconversional analysis of thermal degradation processes.[31,32] It is derived by taking the natural log of eq 4, as shown in eq 5.

$$\ln\left(\frac{\mathrm{d}\alpha}{\mathrm{d}t}\right)_\alpha = \ln[A(\alpha)\,f(\alpha)] - \frac{E_a(\alpha)}{RT(\alpha)} \tag{5}$$

In addition to the rate $(\mathrm{d}\alpha/\mathrm{d}T)$ and reaction model $f(\alpha)$, the activation energy (E_a), pre-exponential factor (A), and temperature (T) are also considered to be dependent on the degree of degradation (α). Where applicable, the respective variables will be denoted as $E_a(\alpha)$, $A(\alpha)$, and $T(\alpha)$ to reflect this. Due to the direct differential treatment of eq 4 utilized by the Friedman method, the resulting experimental rate data can be susceptible to background noise.[19,33] While data smoothing techniques prior to isoconversional analysis can be applied to reduce the error in extracted activation energies,[34] these issues can be avoided by employing an integral solution to the general rate equation for thermal degradation.

At multiple heating rates, eq 4 can be rearranged and integrated to form eq 6.

$$\int_0^\alpha \frac{\mathrm{d}\alpha}{f(\alpha)} = \frac{A}{\beta}\int_0^T \exp\left(-\frac{E_a(\alpha)}{RT(\alpha)}\right)\mathrm{d}T \tag{6}$$

The left-hand side of eq 6 is commonly abbreviated to $g(\alpha)$. Through orthodox model-based kinetic analyses, $g(\alpha)$ could be characterized by integrating the corresponding mechanistic reaction model $f(\alpha)$. The temperature integral on the right-hand side, however, results in an incomplete gamma function which is insolvable in its closed form.[35,36] A range of mathematical approximations to this integral, however, have permitted the development of integral isoconversional methods for the kinetic analyses of thermal processes.[37] The Flynn−Ozawa−Wall (FWO) method is an early and popular integral application of the isoconversional technique,[38] utilizing Doyle's approximation for the temperature integral.[36] A more accurate method proposed by Kissinger−Akahira−Sunose (KAS),[39] is an isoconversional development of a previous method for thermal analysis which originally assumed a constant activation energy.[40] KAS is related to the Coats and Redfern method,[41] as both approaches use the Murray approximation to the temperature integral.[42,43] Through this approximation, eqs 4 and 6 can be combined to form eq 7, which depicts the KAS method for the integral analysis of thermal processes.

$$\ln\left(\frac{\beta}{T(\alpha)^2}\right)_\alpha = -\ln\left[\frac{E_a(\alpha)}{RT(\alpha)}\int_0^\alpha \frac{\mathrm{d}\alpha}{f(\alpha)}\right] - \frac{E_a(\alpha)}{RT(\alpha)} \tag{7}$$

Variations of eq 7 include integral isoconversional methods by Starink[44] and Lyon,[45] which adopt a similar application to the KAS method. Recently, more advanced mathematical approaches by Vyazovkin[46−48] have further produced exact integral solutions without numerical approximation. These methods can reliably predict both isothermal and non-isothermal levels of degradation in the absence of a reaction model $f(\alpha)$ and Arrhenius factor (A).[17] For ease of application and comparison, however, the current study focused on the KAS method for the integral acquisition of activation energy values.

Prediction of Isothermal Degradation. By rearranging and integrating eq 4, the time-dependent isothermal degradation at a specified temperature (T_0) can be predicted. Equation 8 derived by Friedman describes the corresponding execution in the current study.[31,49]

$$t_\alpha = \int_0^\alpha \frac{\exp\left(\frac{E_a(\alpha)}{RT_0}\right)}{[A(\alpha)\,f(\alpha)]}\,\mathrm{d}\alpha \tag{8}$$

The values of the integral with respect to α are calculated using the Friedman-derived activation energies. Values for $A(\alpha)\cdot f(\alpha)$ can be obtained from the y-intercepts of the fitted lines used to obtain the corresponding activation energies. The resulting integral can then be plotted against α and iteratively integrated at increments of $\Delta\alpha = 0.01$ to obtain t_α at the given isothermal temperature (T_0).

EXPERIMENTAL SECTION

Thermogravimetric Analysis (TGA) of SLI. SLI was prepared and isolated to 98% purity in accordance with the methods described previously.[7] Samples of SLI were analyzed using a Mettler Toledo TGA/DSC 1 Thermogravimetric

DOI: 10.1021/acs.iecr.9b00797
Ind. Eng. Chem. Res. 2019, 58, 8112−8122

Analyzer. Then, 3−4 mg of material was weighed to the nearest 0.1 μg using a Mettler Toledo UMX2 Ultra-Microbalance and placed in a 100 μL aluminum crucible with pierced lid. Individual samples were heated from 30 to 550 °C at rates of 5, 10, 20, and 50 °C/min. Sample mass measurements were collected every second to the nearest 0.01 μg. Separate samples were analyzed in air and in N_2 atmospheres to permit the development of individual degradation models for the thermo-oxidative and thermal degradation of SLI. Gas flow was maintained at 50 mL/min throughout all analyses.

Data Processing and Isoconversional Kinetic Analysis. For all TGA-derived nonisothermal degradation data, the mass loss (g) was converted to a degree of degradation (α) using eq 1. Individual sets of Friedman-derived activation energies for $0 < \alpha < 1$ were then calculated for the thermal degradation of SLI in both air and N_2. From the normalized TGA data, the rate ($d\alpha/dT$) was obtained for each run using eq 1, and $\ln(d\alpha/dT)$ was plotted against $1/T$ as a function of the degree of degradation (α) and the one-dimensional gradient in the z-plane was extracted at 0.01 increments of α. These gradient values were subsequently converted to the corresponding activation energies using the gas constant, in accordance with eq 5. Analogous activation energy values were concurrently determined via the Kissinger−Akahira−Sunose (KAS) method using eq 7, where $\ln(\beta/T(\alpha))$ versus $1/T$ was plotted as a function α at the experimental heating rates.

The isothermal degradation of SLI in both air and N_2 was calculated by the Friedman method using eq 8 and the Friedman-derived activation energies. Degradation was predicted at 10 °C intervals between 220 and 280 °C, and the predicted degradation at 5 h was considered to determine the influence of changing synthesis temperatures on degradation levels at the recommended reaction time.[7] To validate the isothermal predictions, samples of SLI were heated from 30 to 240 °C at 50 °C/min and held at 240 °C for 5 h, in accordance with the published synthesis conditions.[7]

Quantitative Evolved Gas Analysis via TGA-FTIR Spectroscopy. A Mettler Toledo TGA/DSC 1 Thermogravimetric Analyzer was connected to a Thermo Scientific Nicolet iS-10 FTIR Spectrometer using a Thermo Scientific Nicolet TGA-IR module. The TGA-FTIR system consisted of a 5 ft. glass-lined stainless-steel transfer line (1/8 in. O.D.). Both the cell and transfer line were heated to 180 °C to minimize condensation. Samples of SLI were heated via TGA from 30 to 550 °C at 10 °C/min. SLI was separately analyzed in both air and N_2 at respective flow rates of 50 mL/min. Prior to heating, the TGA gas was purged for 30 min for the acquisition of a representative background FTIR spectrum. Sample spectra were then measured at 36 s intervals, via 36 consecutive scans between 500 and 4000 cm^{-1}, for the duration of the heat cycle. Species of interest were identified using the Nicolet FT-IR Vapor Phase Spectral Library from Thermo Scientific. The five most abundant species in each sample were then quantified via their respective characteristic bands using the Chemigram function in the Thermo Scientific OMNIC Series package.

RESULTS AND DISCUSSION

Thermogravimetric Analysis (TGA) of SLI. The selected temperatures and heating rates for the TGA analysis of SLI were representative of the conditions utilized for previous isoconversional studies on chemically similar organic esters.[50,51] Figure 2 depicts the DTG data of the resulting experiments.

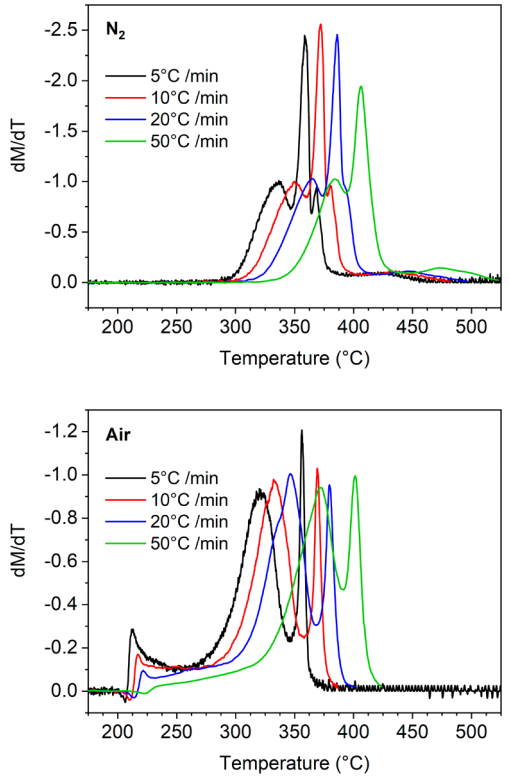

Figure 2. Differential DTG data for the degradation of SLI in N_2 (top) and air (bottom) at heating rates of 5, 10, 20, and 50 °C/min. For dM/dT, M = mass loss (%) and T = temperature (°C).

SLI was found to exhibit three distinct degradation zones in air, while the inert system (N_2) displayed an additional fourth zone during the latter stages of the studied temperature range. (Figure S3). After the final degradation zone, a period of thermal stability ($dM/dT \approx 0$) was observed at all heating rates in both air and N_2. Coupled with the reproducible thermal behavior across different heating rates, this provided a robust window in which the data could be normalized and processed for isoconversional analysis. Mass loss (%) data was normalized in terms of the degree of degradation (α) where the end of the final degradation zone was designated as $\alpha = 1$. Example data is shown Figure S3. Onset temperatures of specific degradation zones, as well as the endset temperatures utilized for mass normalization are provided in Table S1 of the Supporting Information. In this context, the terms onset and endset correspond to temperatures at which degradation processes commence and conclude, respectively.

A high-temperature degradation study of SDS reported a residual mass of 35 wt % following pyrolysis at 700 °C in N_2.[52] Although the maximum temperatures in the current study were 550 °C, post-analysis of the crucibles showed similar black residues to those described in the SDS study, with comparable mass losses. The degradation onset of SLI in N_2 was found to be 348 °C at 50 °C/min and lower than that of SDS, where the decomposition temperature was reported to be 380 °C.[15] The synthesized SLI displayed a strong dependence on heating rate, with a much lower decomposition onset of 300 °C observed at 5 °C/min (N_2). In air, there was less variation in degradation onset temperature with values between 206 and 222 °C at the

DOI: 10.1021/acs.iecr.9b00797
Ind. Eng. Chem. Res. 2019, 58, 8112−8122

experimental heating rates of 5−50 °C/min, respectively. The melting point of SLI was reported as 225 °C when heated at 1 °C/min.[7] The commencement of degradation was not considered to be significantly influenced by melting, as mass loss was observed below this temperature at all experimental heating rates; α = 1 at equilibrium was estimated to correspond to masses of 26.7 and 46.4 wt % in N_2 and air, respectively, see section 1.3 in the Supporting Information for further information.

The difference between degradation in air and N_2 correlates with Vyazokin's postulation that thermo-oxidative degradation typically occurs at approximately 100 °C below the analogous process in an inert atmosphere.[53] Prior to degradation onsets, the observed SLI mass loss before 180 °C in air and 280 °C in N_2 was less than 0.2 wt %, indicating a minimal presence of retained water in SLI under ambient conditions.

Isoconversional Kinetic Analysis. Differential Friedman and integral KAS models were used to obtain the change in E_a as a function of the degree of degradation (α) in both air and N_2. An example plot of the gradients used to determine the activation energies via the Friedman method is shown in Figure 3.

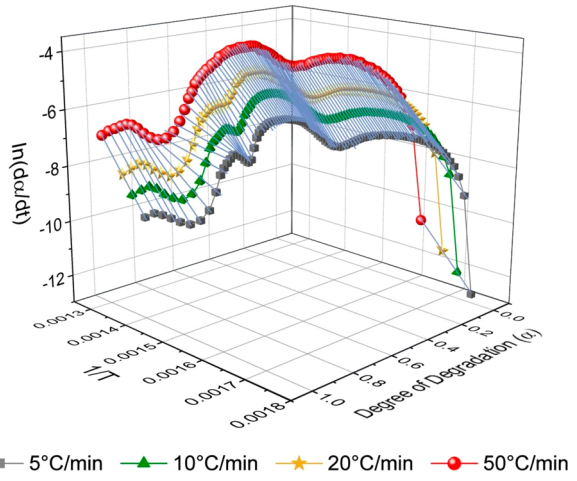

Figure 3. Activation energies obtained via the Friedman differential method of isoconversional kinetic analysis. The data depicts $\ln(d\alpha/dT)$ vs $1/T$ vs α for the degradation of SLI in N_2 at heating rates of 5, 10, 20, and 50 °C/min. Gradients in the z-plane (blue lines) correspond to the activation energy at the given degree of degradation (α); see eq 5.

The corresponding activation energies obtained by both isoconversional methods, in air and N_2, are displayed in Figure 4.

In N_2, environmental changes in E_a were found to approximately coincide with the different degradation zones, see Table S1 for tangential onset data. The activation energies between α = 0 and 1 from the Friedman and KAS models were found to correlate well with each other, with average values of 150.1 and 149.1 kJ/mol, respectively. Renewably sourced biofuels exhibit some chemical similarity to SLI, with a common presence of alkyl chains, as well as a prevalence of C−C, C−O, and C═O bonds. The triglyceride systems exhibited similar average Friedman values of 124[50] and 167 kJ/mol,[54] respectively. The reported degradation onsets of ∼300 °C for these species were also similar to those observed in the current study and much higher than the corresponding methyl esters

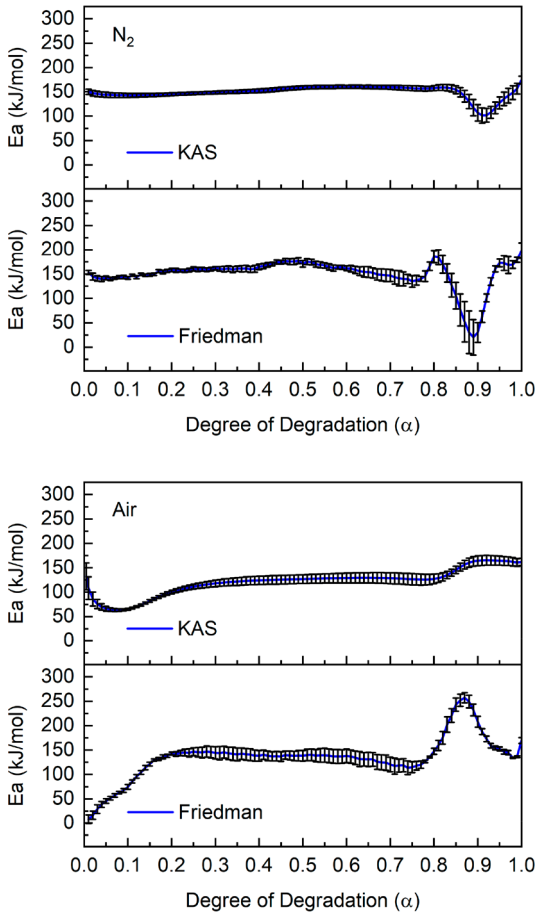

Figure 4. Change in activation energy for the thermal and thermo-oxidative degradation of SLI in N_2 (top) and air (bottom). Values were obtained using the Friedman and KAS isoconversional kinetic models. Error bars correspond to the error in the respective regression fits used to calculate energies. Activation energy values are provided in Tables S2−S4.

where decomposition commenced between 100 and 150 °C.[50,54] This may suggest that the additional electron density donated by the isethionate group, when compared to that of a methyl group, stabilizes the ester bond similar to the glycerol group and fatty acid chains in the triglyceride system, thus resulting in a greater thermal stability in an inert atmosphere.

In the oxidative air environment, average activation energy values between α = 0 and 1 were calculated to be 135.6 and 120.8 kJ/mol using the Friedman and KAS models, respectively. A drop in the activation energy compared to the inert process expectedly results in lower degradation onset temperatures.[55] While activation energy values provide an insight into thermal decomposition behavior, the degradation rate is also dependent on the pre-exponential factor A. Friedman values of $\ln [A(\alpha)\cdot f(\alpha)]$ have been calculated for predictive purposes, whereas the physical meaning of the standalone factor A has been reported to be inconclusive in the context of isoconversional kinetics.[56,57]

In both the N_2 and air environments, Figure 4 shows how the data obtained by the Friedman method appears noisier than the data obtained by KAS. As the former method directly differentiates the general rate equation, it typically produces a greater fluctuation in calculated E_a values.[53] While data smoothing filters are common,[42] they were not utilized as the majority of R^2 values relating to Friedman E_a values were

DOI: 10.1021/acs.iecr.9b00797
Ind. Eng. Chem. Res. 2019, 58, 8112−8122

greater than 0.98 and therefore deemed reliable (see Tables S2–S4 for full data). Although the R^2 values obtained using KAS exhibit more instances greater than 0.99, the approximations inherent to this integral method can introduce a systematic error into any obtained kinetic parameters.[17] The KAS model has also been shown to exhibit poorer predictive capabilities over an analogous Friedman model.[33] For these reasons, the Friedman method was preferred and utilized to predict the isothermal degradation of SLI.

Predicted Isothermal Degradation. The experimentally derived Friedman isoconversional degradation parameters and their corresponding models were used to determine the effect of changing process conditions on the degradation of SLI. A published synthesis of SLI reports an esterification temperature of 240 °C, with a total process time of 5 h.[7] Predicted degradation isotherms were therefore produced at temperatures between 220 and 280 °C; see Figure 5.

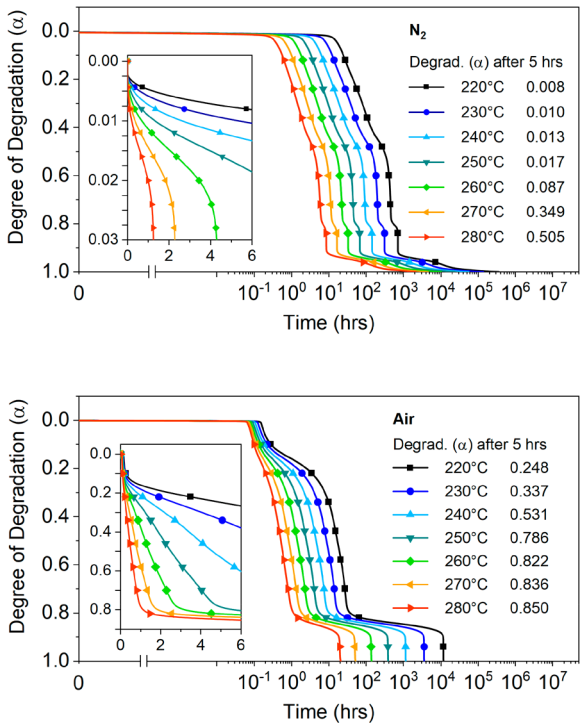

Figure 5. Predicted isothermal degradation of SLI in N_2 (top) and air (bottom) from exposure to sustained temperatures between 220 and 280 °C. Inset shows the initial stages of degradation, where the inset *x*-axis represents time (h) on a linear scale. Note the difference in the *y*-scales between the air and N_2 data. Degree of degradation (α) was obtained from the respective Friedman activation energies using eq 8. Legend displays predicted degradation (α) after 5 h of isothermal exposure.

In the N_2 system, degradation after 5 h at 240 °C was found to be 0.013 (α), which equates to 1.0 wt % of the total SLI mass in physical terms. The degradation levels at 220 and 230 °C were 0.008 and 0.010, respectively. The esterification rate during the manufacture of SLI is reported to drop significantly when the reaction temperature is lowered below 230 °C.[10] Decreasing the process temperature therefore may not decrease the process-induced thermal degradation, since the increase in reaction times required for an equivalent level of esterification, may offset the observed improvements in stability. At 260 °C, there is a 530% increase in the degradation level over 5 h compared to 240 °C, which increases to >2800% at 270 °C. In N_2, the ideal parameters for optimizing the reaction rate while minimizing decomposition therefore resides between 240 and 250 °C.

In air, degradation levels at equivalent temperatures were found to be significantly higher than those observed in the N_2 environment. At 240 °C, the predicted degradation after 5 h (α = 0.531) equated to 28.5 wt % of mass loss. While a reduced operating temperature of 220 °C is predicted to significantly decrease degradation to a mass loss of 13.3 wt %, these degradation levels would still be substantially higher than those for the inert system. Catalytic isethionate synthesis routes can be operated at temperatures as low as 200 °C,[58] but an analysis of the degradation data indicates that mass loss is still predicted to be 9.5 wt % over 5 h. On the basis of these observations, it becomes clear that any process involving the high-temperature esterification of SLI should be operated within a rigidly controlled inert atmosphere in order to minimize yield loss to thermal degradation.

While long-chain organic molecules similar to SLI have previously been studied by isoconversional methods,[50,51,54] the predicted isotherms were nevertheless compared with experimental isotherms to verify the applicability of the Friedman model to this particular system. SLI was heated to 240 °C for 5 h to simulate published synthesis conditions, and the mass was observed via TGA.[7] The resulting plots of mass loss in both air and N_2 atmospheres, together with their nonisothermally derived predictions, are shown in Figure 6.

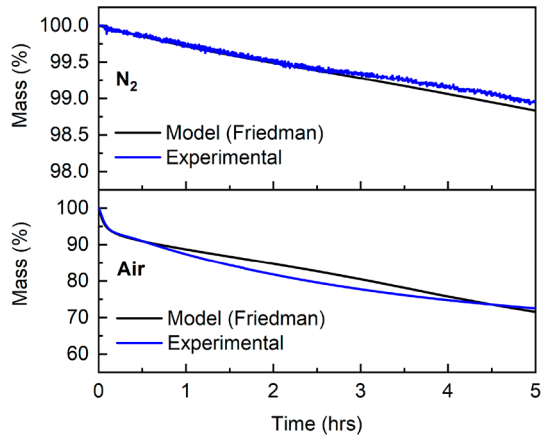

Figure 6. Experimental isothermal TGA plots of SLI in N_2 (top) and air (bottom) compared with the predicted model isotherms. Samples were heated to 240 °C for 5 h to simulate the synthesis conditions for SLI.[7] Model isotherms were generated from nonisothermally derived Friedman models.

After 5 h at 240 °C the measured degradation in air was substantially higher than N_2 with respective mass loss values of 28.9 and 1.1 wt %. While the experimental data showed good agreement to the predicted data, deviations around 2.5 h in air and 4 h in N_2 were respectively observed. The associated differences between the observed and experimental mass losses were 3.0 and 0.1 wt % in air and N_2, respectively. The underestimation in air could have resulted from increasing inaccuracies in the corresponding isoconversional model. The R^2 values associated with the derivation of the corresponding activation energies are provided in Table S4. While values were predominantly greater than 0.99 in the early stages of the

DOI: 10.1021/acs.iecr.9b00797
Ind. Eng. Chem. Res. 2019, 58, 8112−8122

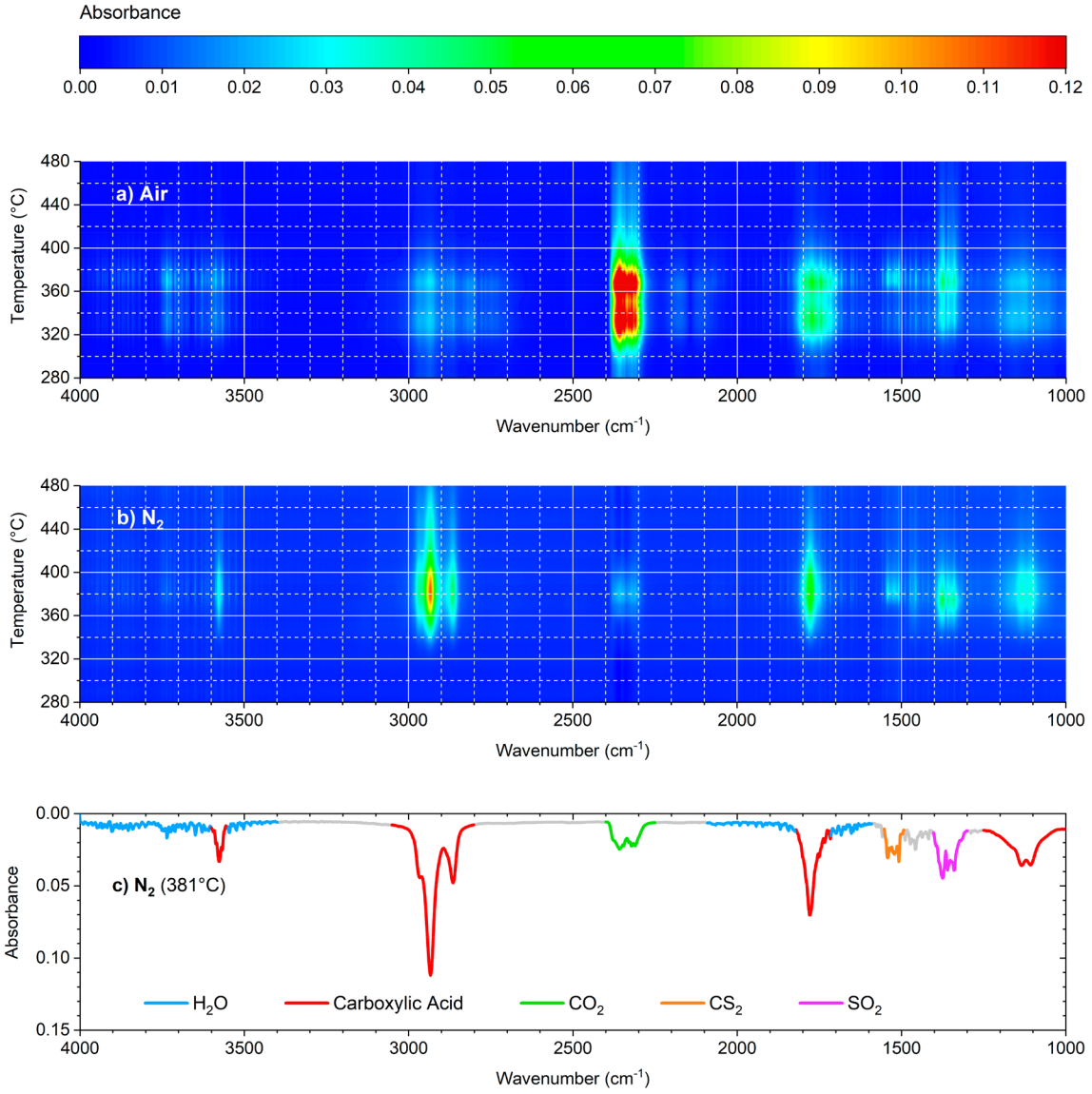

Figure 7. Color maps depicting the evolved gases measured via TGA-FTIR during the thermal degradation of SLI in (a) air and (b) N_2. Color scale corresponds to the FTIR absorbance of evolved species at the corresponding temperature and wavenumber. Samples were heated from 30 to 550 °C at 10 °C/min. The complete FTIR data set is shown in Figure S6. (c) Single FTIR spectrum of the evolved gases in N_2 at 381 °C. Legend depicts the five most abundant species. Library spectra used to identify species of interest can be found in Figure S5.

degradation process, a decrease to 0.98 is observed beyond α = 0.20. The resulting increase in error for the Friedman-derived activation energies in air is also presented in Figure 4. While this error has manifested itself as a minor deviation in mass over the time scales presented in Figure 6, a greater error in the E_a values is observed at higher degrees of degradation (α > 0.75), particularly in the inert system. As this could significantly impact the predictive capability of these models, their application at greater levels of degradation (α > 0.75) is not recommended.

TGA-FTIR Analysis of SLI. Data from the TGA-FTIR analysis, conducted to identify the volatile products released from the decomposition of SLI, is shown in Figure 7.

The maximum total absorbance was measured at 381 °C in N_2 and 369 °C in air. At these temperatures, all significant absorption bands were detected and the resulting single FTIR spectra were therefore considered to be representative of the gases produced in each system. A small time delay was expected between gas evolution in the TGA furnace and subsequent detection via the FTIR spectrometer. Given the combined volume of the furnace, transfer line, and spectrometer cell, this delay is not considered to exceed the FTIR measurement interval at the experimental purge gas flow rate. Through comparison with library spectra, the five most spectroscopically abundant species from the thermal degradation of SLI were identified, as shown in Figure 7c. The temperature-dependent data (Figures 7a,b) showed that while the relative amounts of each gas differed with a change in degradation atmosphere, both the N_2 and air systems exhibited the same five gaseous species in highest quantity. The literature values used to identify and confirm these gaseous species are provided in Table 1. The specific vibrations corresponding to each band were determined where possible.

From Table 1, the single bands attributed to sulfur dioxide (SO_2), carbon disulfide (CS_2), carbon dioxide (CO_2), and water vapor (H_2O) were distinctive, characteristic, and easily

DOI: 10.1021/acs.iecr.9b00797
Ind. Eng. Chem. Res. 2019, 58, 8112−8122

Table 1. Literature Values for FTIR Peaks Characteristic of Materials Identified via the Evolved Gas Analysis of SLI

material	vibrational mode	bond	wavenumber (cm^{-1})[a]
SO_2	asymmetric stretch (ν_3)	O=S=O	1320–1395[59]
CS_2	asymmetric stretch (ν_3)	S=C=S	1523[60]
CO_2	asymmetric stretch (ν_3)	O=C=O	2349[61]
	asymmetric stretch (ν_3)	O–H–O	3755[61]
H_2O	symmetric stretch (ν_1)	O–H–O	3651[61]
	symmetric bend (ν_2)	O–H–O	1595[61]
lauric acid[62]	carboxylic acid stretch	C=O	1777[63]
	alkyl stretches[b]	C–H	2840–2975[64]
	carboxylic acid stretch	O–H	3575[63]
	skeletal stretch	C–C	1040–1175[62]

[a]Where single values are provided, the wavenumber corresponds to a peak value quoted in the literature. [b]See Hill et al. for detailed saturated acid peak assignments.[64]

attributable to the respective species. Carboxylic acids are common products in both the oxidative and inert thermal degradation of alkyl esters, formed via hydrolysis and intramolecular rearrangement.[65,66] As the experimental FTIR peaks displayed very strong correlation with vapor spectra of acid homologues,[67] the remaining peaks in Figure 7c have been attributed to linear saturated carboxylic acids. Contrary to the dimeric condensed phase of carboxylic acids, vapor species typically exist in the monomeric form. This results in significant shifts to the IR stretching frequencies of C=O and O–H, which otherwise contribute to hydrogen bonding interactions.[63] The observed C=O (1777 cm^{-1}) and O–H (3576 cm^{-1}) bands were characteristic of vapor-phase carboxylic acids and correlate very well with their respective literature peak widths and wavenumber values of 1777 and 3575 cm^{-1}.[63,67] Analogous thermal degradation studies of similar lipids also report evolutions of alcohols, esters, and aldehydes.[50,51,68] Primary, secondary, and tertiary alcohol stretches typically occur between 3640 and 3670 cm^{-1} in the vapor phase.[63] Despite the large quantities of alcohol detected in the pyrolysis of SDS,[16] there is no significant evidence of this for SLI in air or N_2. Using the Beer–Lambert law, the intensity ratio measured between C=O and O–H in the displayed spectrum was found to be similar to that of a reference carboxylic acid spectrum.[63] However, a slight excess in C=O absorbance is consistent with the presence of additional carbonyl species such as aldehydes and ketones.

Quantitative Analysis of Evolved Gases. To quantify gas evolution as a function of degradation, the change in absorbance for each of the characteristic bands (identified in Figure 7c) were plotted as a function of temperature. While carboxylic acids were identified as the primary carbonyl constituent, decomposition within the alkyl chains was also likely to result from oxidative combustion, resulting in the evolution of independent alkyl fragments.[54,69] The alkyl and carbonyl bands were therefore integrated individually to determine the relative quantities of each functional group.

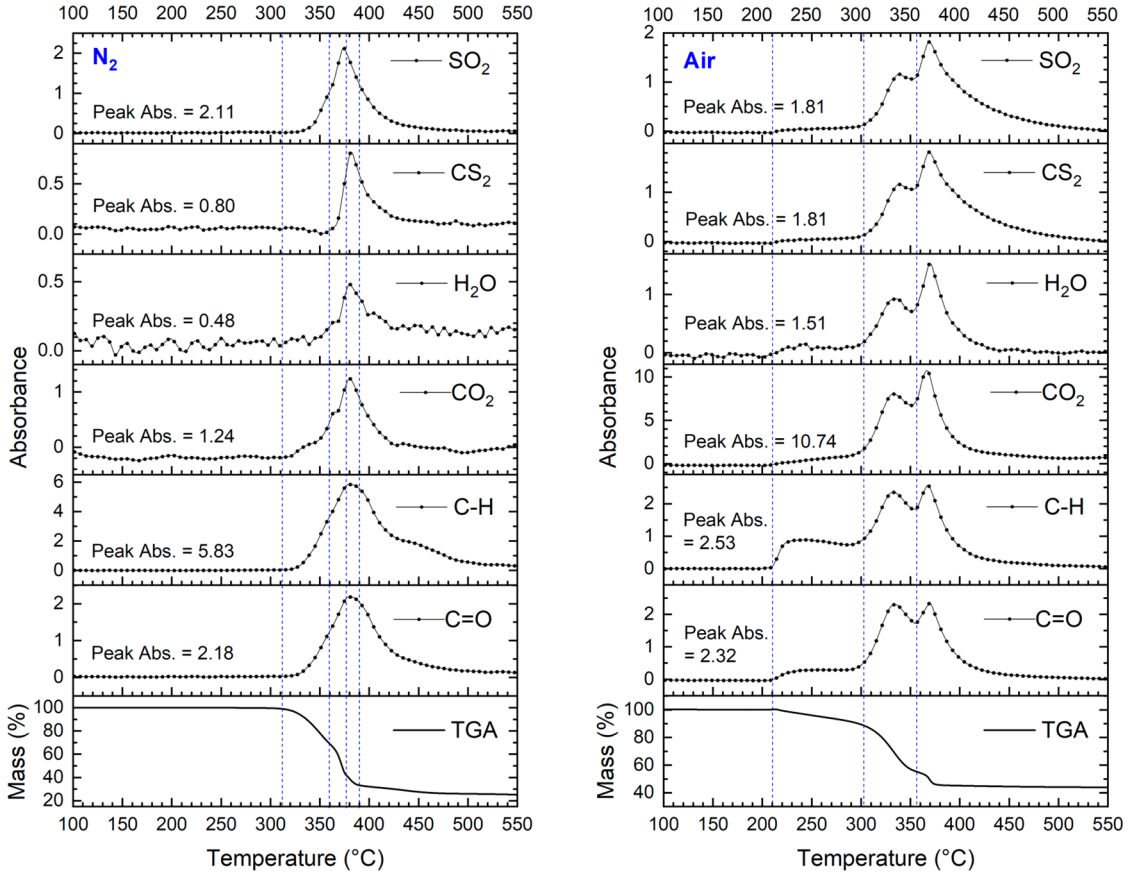

Figure 8. Absorbance of the characteristic FTIR bands of the evolved gas during the thermal decomposition of SLI in N_2 (left) and air (right). SLI samples were heated to 550 °C at 10 °C/min. Dashed lines represent the onset of degradation zones 1–4 (where applicable) as measured via TGA. The corresponding TGA data at 10 °C/min is also provided. All measured transition temperatures are shown in full in Table S1.

DOI: 10.1021/acs.iecr.9b00797
Ind. Eng. Chem. Res. 2019, 58, 8112–8122

The resulting temperature-dependent absorptions in both air and N_2 atmospheres are shown in Figure 8.

In both air and N_2, the temperatures at which changes in absorption occur, coincide with the degradation zones identified via the differential TGA analysis (Figure 2). See Table S1 for further data. Due to the inherent interdependencies between radical reactions, the measured species in each environment display comparable maxima with broadly similar evolution trends with respect to temperature. These shared temperature-dependent inclinations across gaseous species correspond with previous studies pertaining to similar methods and molecules.[51,68,70]

The significant evolutions of alkyl species, carboxylic acids, CO_2, and water vapor correspond with the gases produced from the thermal degradation of other long-chain organic molecules.[50,54,68,71] A decompositional study of SDS reported that the surfactant degraded to form primary alkenes, with characteristic C=C vinyl stretches and general olefinic stretch reported to occur at 1640 and 1580 cm^{-1}, respectively.[62] In the current study, the experimental spectra displayed very limited activity in these regions to confirm any substantial formation of volatile alkenes in the inert thermal degradation of SLI (Figure 7a). The observed evolutions of SO_2 correspond with those reported for the thermal decomposition of alkyl sulfonated surfactants,[72] as well as SDS.[52] CS_2 is a less commonly reported degradation product of organic species. However, its presence in this study was confirmed by comparison with reference spectra and literature values of characteristic bands.[60] Significant increases in CO_2 and water vapor absorption were observed in air when compared to the inert system. In reported evolved gas studies of long-chain organic materials, similar increases have been proposed to result from oxidative combustion, particularly at the temperatures corresponding to the second and third degradation zones observed in the oxidative study of SLI (Figure 8).[68,73] However, due to the highly complex, interdependent nature of the radical reactions pertaining to all evolved gases observed in this study, further time-resolved analyses would be required to confirm the specific mechanisms most relevant to the thermal degradation of isethionate surfactants.

CONCLUSIONS

The thermal degradation of sodium lauroyl isethionate (SLI) was measured using TGA and analyzed via isoconversional kinetic methods. Dynamic experiments resulted in degradation onset temperatures of 300 and 208 °C in air and N_2, respectively, both of which were lower than the 380 °C reported for sodium dodecyl sulfate.[15] Differential Friedman-derived activation energies were used to predict isothermal degradation levels under typical isethionate manufacturing conditions. Thoroughly inert synthesis conditions are recommended for isethionate production, after experimentally verified data indicated that SLI degradation levels were 28 times higher in air than N_2 at published synthesis temperatures of 240 °C.[7] Previous patent literature reported elevated SLI decomposition at temperatures higher than 220 °C.[13] From the results in the current study, isethionate synthesis temperatures could be increased to 250 °C under strictly inert manufacturing conditions, given that significant increases in degradation levels were not predicted until 260 °C. Gradual heating of the reaction vessel would be advocated to avoid exceeding desired temperatures, thus maximizing product activity levels,[13] color[10] and odor[14] by minimizing degradation. Despite the current focus on a high-temperature catalyst-free manufacturing process, the versatility of the obtained Friedman models permit the prediction of degradation resulting from any dynamic or isothermal temperature exposure,[33] thus extending their applicability to alternative processes pertaining to SLI manufacture. Even with increasing applications of isoconversional kinetics in the thermal analysis of biorenewable organic fuels,[50,51] the methods were seldom utilized in the study of ionic surfactant systems. The correlation between predicted and measured degradation in this study supports their utilization in analysis of more complex organic systems, where metallic associations lead to a greater complexity in atomic composition, polarity and columbic interactions.

A real-time TGA-FTIR analysis was conducted to identify and quantify the gases produced through the thermal degradation of SLI. The analysis revealed evolutions of carbon dioxide, carbon disulfide, sulfur dioxide, water vapor, and organic fragments. In addition to improving product properties, managing degradation levels through the temperature-dependent presence of characteristic FTIR bands, would also reduce the risk of the observed toxic, pungent sulfurous emissions.[74] Walele et al. reported that activity levels of commercial isethionate esters varies between 78 and 85%,[10] which correlates with previous reviews of isethionate ester manufacture.[58] In order to determine if the upper limits on this range result from limited product stability, future work could utilize the models generated in this study to correlate product activity levels with decomposition of SLI. By associating activity levels with desired levels of product performance, the resulting material lifetimes could be used to optimize SLI manufacturing processes for acceptable levels of thermal degradation.

ASSOCIATED CONTENT

Supporting Information

The Supporting Information is available free of charge on the ACS Publications website at DOI: 10.1021/acs.iecr.9b00797.

Raw TGA data, degradation step temperatures, tabulated isoconversional kinetic data and TGA-FTIR data (PDF)

AUTHOR INFORMATION

Corresponding Author

*E-mail: cm09mij@leeds.ac.uk.

ORCID

Mohammed I. Jeraal: 0000-0001-9111-7404

David Harbottle: 0000-0002-0169-517X

Notes

The authors declare no competing financial interest.

ACKNOWLEDGMENTS

This research was completed at the EPSRC Centre for Doctoral Training in Complex Particulate Products and Processes (EP/L015285/1), in collaboration with Innospec Ltd., who we gratefully acknowledge for their support of this work. We also thank Adrian Cunliffe and Karine Alves Thorne at the University of Leeds for analytical support.

REFERENCES

(1) Rieger, M.; Rhein, L. D. *Surfactants in Cosmetics.*; Marcel Dekker: New York, 1997.

(2) Petter, P. J. Fatty acid sulphoalkyl amides and esters as cosmetic surfactants. *Int. J. Cosmet. Sci.* **1984**, *6* (5), 249–260.

(3) Ananthapadmanabhan, K.; Yang, L.; Vincent, C.; Tsaur, L.; Vetro, K. M.; Foy, V.; Zhang, S.; Ashkenazi, A.; Pashkovski, E.; Subramanian, V. A Novel Technology in Mild and Moisturizing Cleansing Liquids. *Cosmet. Derm.* **2009**, *22* (6), 307−316.
(4) Wilson, D.; Berardesca, E.; Maibach, H. I. In vivo transepidermal water loss and skin surface hydration in assessment of moisturization and soap effects. *Int. J. Cosmet. Sci.* **1988**, *10* (5), 201−211.
(5) Ananthapadmanabhan, K.; Yu, K.; Meyers, C.; Aronson, M. Binding of surfactants to stratum corneum. *J. Soc. Cosmet. Chem.* **1996**, *47* (4), 185−200.
(6) Friedman, M.; Wolf, R. Chemistry of soaps and detergents: Various types of commercial products and their ingredients. *Clin. Dermatol.* **1996**, *14* (1), 7−13.
(7) Jeraal, M. I.; Roberts, K. J.; McRobbie, I.; Harbottle, D. Process-Focused Synthesis, Crystallization, and Physicochemical Characterization of Sodium Lauroyl Isethionate. *ACS Sustainable Chem. Eng.* **2018**, *6* (2), 2667−2675.
(8) Cahn, A.; Haass, R. A.; Lamberti, V. Preparation of sulfonated fatty acid ester surface-active agents. U.S. Patent 3320292A, 1967.
(9) Holland, F. A.; Kelly, W. A.; Mccrimlisk, G. J. Process for the continuous production of fatty acid esters of hydroxy sulfonates. U.S. Patent 3420857A, 1969.
(10) Walele, I. I.; Syed, S. A. Fatty acid esters of hydroxyalkyl sulfonate salts and process for producing same. U.S. Patent 6069262A, 2000.
(11) Holt, E. K.; Mueller, H. H.; Urban, W. J. Process for preparing hydroxy sulfonate esters. U.S. Patent 3429136A, 1968.
(12) McCrimlisk, G. J. Process for the production of fatty acid esters of hydroxy sulfonates. U.S. Patent 3420858A, 1969.
(13) Login, R. B.; Walele, I. I.; Otterson, R. J. Process for the production of fatty acid esters of hydroxyalkyl sulfonate salts. U.S. Patent 4515721A1985.
(14) Lamberti, V.; Boen, L. K. Process for producing directly esterified fatty acyl isethionate by a mixed zinc oxide-sulfonic acid catalyst. U.S. Patent 4405526A, 1983.
(15) Chernikov, O. I.; Glagolev, R. V.; Zvyagina, T. I. Thermostability of surfactants having various chemical structures. *J. Appl. Chem. USSR* **1983**, *56* (6), 1347−1349.
(16) Liddicoet, T. H.; Smithson, L. H. Analysis of surfactants using pyrolysis-gas chromatography. *J. Am. Oil Chem. Soc.* **1965**, *42* (13), 1097−1102.
(17) Vyazovkin, S. *Isoconversional Kinetics of Thermally Stimulated Processes*.; Springer International Publishing, 2016.
(18) Flynn, J. H. A critique of lifetime prediction of polymers by thermal analysis. *J. Therm. Anal.* **1995**, *44* (2), 499−512.
(19) Vyazovkin, S.; Wight, C. A. Isothermal and non-isothermal kinetics of thermally stimulated reactions of solids. *Int. Rev. Phys. Chem.* **1998**, *17* (3), 407−433.
(20) Vyazovkin, S.; Burnham, A. K.; Criado, J. M.; Pérez-Maqueda, L. A.; Popescu, C.; Sbirrazzuoli, N. ICTAC Kinetics Committee recommendations for performing kinetic computations on thermal analysis data. *Thermochim. Acta* **2011**, *520* (1), 1−19.
(21) Vyazovkin, S.; Chrissafis, K.; Di Lorenzo, M. L.; Koga, N.; Pijolat, M.; Roduit, B.; Sbirrazzuoli, N.; Suñol, J. J. ICTAC Kinetics Committee recommendations for collecting experimental thermal analysis data for kinetic computations. *Thermochim. Acta* **2014**, *590*, 1−23.
(22) White, D. R.; White, R. L. Isoconversion Effective Activation Energy Profiles by Variable Temperature Diffuse Reflection Infrared Spectroscopy. *Appl. Spectrosc.* **2008**, *62* (1), 116−120.
(23) Bonnet, E.; White, R. L. Species-specific isoconversion effective activation energies derived by thermogravimetry-mass spectrometry. *Thermochim. Acta* **1998**, *311* (1), 81−86.
(24) Madbouly, S. A.; Otaigbe, J. U. Kinetic Analysis of Fractal Gel Formation in Waterborne Polyurethane Dispersions Undergoing High Deformation Flows. *Macromolecules* **2006**, *39* (12), 4144−4151.
(25) Farjas, J.; Roura, P. Isoconversional analysis of solid state transformations (Part I. Single step transformations with constant activation energy). *J. Therm. Anal. Calorim.* **2011**, *105* (3), 757−766.
(26) Criado, J. M.; Ortega, A.; Gotor, F. Correlation between the shape of controlled-rate thermal analysis curves and the kinetics of solid-state reactions. *Thermochim. Acta* **1990**, *157* (1), 171−179.
(27) Vyazovkin, S. *Modern Isoconversional Kinetics: From Misconceptions to Advances*; Elsevier Science, 2018; Vol. *6*.
(28) Vyazovkin, S. Isoconversional Kinetics of Polymers: The Decade Past. *Macromol. Rapid Commun.* **2017**, *38* (3), 1600615.
(29) Vyazovkin, S. Kinetic concepts of thermally stimulated reactions in solids: A view from a historical perspective. *Int. Rev. Phys. Chem.* **2000**, *19* (1), 45−60.
(30) Vyazovkin, S. A time to search: finding the meaning of variable activation energy. *Phys. Chem. Chem. Phys.* **2016**, *18* (28), 18643−18656.
(31) Friedman, H. L. Kinetics of thermal degradation of char-forming plastics from thermogravimetry. Application to a phenolic plastic. *J. Polym. Sci., Part C: Polym. Symp.* **1964**, *6* (1), 183−195.
(32) Burnham, A. K.; Dinh, L. N. A comparison of isoconversional and model-fitting approaches to kinetic parameter estimation and application predictions. *J. Therm. Anal. Calorim.* **2007**, *89* (2), 479−490.
(33) Berčič, G. The universality of Friedman's isoconversional analysis results in a model-less prediction of thermodegradation profiles. *Thermochim. Acta* **2017**, *650*, 1−7.
(34) Zhang, X.; de Jong, W.; Preto, F. Estimating kinetic parameters in TGA using B-spline smoothing and the Friedman method. *Biomass Bioenergy* **2009**, *33* (10), 1435−1441.
(35) Madhusudanan, P. M.; Krishnan, K.; Ninan, K. N. New approximation for the p(x) function in the evaluation of non-isothermal kinetic data. *Thermochim. Acta* **1986**, *97*, 189−201.
(36) Doyle, C. D. Series Approximations to the Equation of Thermogravimetric Data. *Nature* **1965**, *207*, 290.
(37) Flynn, J. H. The 'Temperature Integral' — Its use and abuse. *Thermochim. Acta* **1997**, *300* (1), 83−92.
(38) Flynn, J. H.; Wall, L. A. A quick, direct method for the determination of activation energy from thermogravimetric data. *J. Polym. Sci., Part B: Polym. Lett.* **1966**, *4* (5), 323−328.
(39) Akahira, T.; Sunose, T. Method of determining activation deterioration constant of electrical insulating materials. *Res. Rep. Chiba Inst. Technol.* **1971**, *16*, 22−31.
(40) Kissinger, H. E. Reaction Kinetics in Differential Thermal Analysis. *Anal. Chem.* **1957**, *29* (11), 1702−1706.
(41) Coats, A. W.; Redfern, J. P. Kinetic Parameters from Thermogravimetric Data. *Nature* **1964**, *201*, 68.
(42) Farjas, J.; Roura, P. Isoconversional analysis of solid state transformations (Part II. Complex transformations). *J. Therm. Anal. Calorim.* **2011**, *105* (3), 767−773.
(43) Murray, P.; White, J. Kinetics of the thermal dehydration of clays. (Part IV: Interpretation of the differential thermal analysis of the clay minerals). *Trans. Brit. Ceram. Soc.* **1955**, *54*, 204−238.
(44) Starink, M. J. A new method for the derivation of activation energies from experiments performed at constant heating rate. *Thermochim. Acta* **1996**, *288* (1), 97−104.
(45) Lyon, R. E. An integral method of nonisothermal kinetic analysis. *Thermochim. Acta* **1997**, *297* (1), 117−124.
(46) Vyazovkin, S.; Dollimore, D. Linear and Nonlinear Procedures in Isoconversional Computations of the Activation Energy of Nonisothermal Reactions in Solids. *J. Chem. Inf. Model.* **1996**, *36* (1), 42−45.
(47) Vyazovkin, S. Evaluation of activation energy of thermally stimulated solid-state reactions under arbitrary variation of temperature. *J. Comput. Chem.* **1997**, *18* (3), 393−402.
(48) Vyazovkin, S. Advanced isoconversional method. *J. Therm. Anal. Calorim.* **1997**, *49* (3), 1493−1499.
(49) Wang, J.; Laborie, M.-P. G.; Wolcott, M. P. Comparison of model-free kinetic methods for modeling the cure kinetics of commercial phenol-formaldehyde resins. *Thermochim. Acta* **2005**, *439* (1), 68−73.
(50) Li, H.; Niu, S.; Lu, C.; Wang, Y. Comprehensive Investigation of the Thermal Degradation Characteristics of Biodiesel and Its

DOI: 10.1021/acs.iecr.9b00797
Ind. Eng. Chem. Res. 2019, 58, 8112−8122

Feedstock Oil through TGA-FTIR. *Energy Fuels* **2015**, *29* (8), 5145−5153.
(51) Li, H.; Niu, S.; Lu, C.; Cheng, S. Comparative evaluation of thermal degradation for biodiesels derived from various feedstocks through transesterification. *Energy Convers. Manage.* **2015**, *98*, 81−88.
(52) Patterson, J. M.; Kortylewicz, Z.; Smith, W. T. Thermal degradation of sodium dodecyl sulfate. *J. Agric. Food Chem.* **1984**, *32* (4), 782−784.
(53) Vyazovkin, S.; Sbirrazzuoli, N. Isoconversional Kinetic Analysis of Thermally Stimulated Processes in Polymers. *Macromol. Rapid Commun.* **2006**, *27* (18), 1515−1532.
(54) Reshad, A. S.; Tiwari, P.; Goud, V. V. Thermal Degradation Kinetic Study of Rubber Seed Oil and Its Methyl Esters under Inert Atmosphere. *Energy Fuels* **2017**, *31* (9), 9642−9651.
(55) Vyazovkin, S. Model-free kinetics. *J. Therm. Anal. Calorim.* **2006**, *83* (1), 45−51.
(56) Sestsk, J.; Stulikova, M. *Thermophysical Properties of Solids: Their Measurements and Theoretical Thermal Analysis*; Elsevier: Amsterdam, 1984.
(57) Pielichowski, K. Kinetic analysis of the thermal decomposition of polyaniline. *Solid State Ionics* **1997**, *104* (1), 123−132.
(58) Friedman, M.; Spitz, L. Chemistry, Formulation, and Performance of Syndet and Combo Bars. *Soap Manufacturing Technology* **2016**, 73.
(59) Petruci, J. F.; Wilk, A.; Cardoso, A. A.; Mizaikoff, B. Online Analysis of H2S and SO2 via Advanced Mid-Infrared Gas Sensors. *Anal. Chem.* **2015**, *87* (19), 9605−9611.
(60) Bhagavantam, S. The Infrared and Raman Spectra of CS2. *Phys. Rev.* **1932**, *39* (6), 1020−1020.
(61) Ritland, H. N. *Technical Report: The Infrared Absorption Spectrum of Water Vapor and Carbon Dioxide*; Lockheed Information Systems Laboratory, 1962.
(62) Socrates, G. *Infrared and Raman Characteristic Group Frequencies: Tables and Charts*; Wiley: Chichester, U.K., 2004.
(63) Welti, D. *Infrared Vapour Spectra.*; Heyden & Son: London, 1970.
(64) Hill, I. R.; Levin, I. W. Vibrational spectra and carbon-hydrogen stretching mode assignments for a series of n-alkyl carboxylic acids. *J. Chem. Phys.* **1979**, *70* (2), 842−851.
(65) Alexander, R.; Kralert, P. G.; Kagi, R. I. Kinetics and mechanism of the thermal decomposition of esters in sediments. *Org. Geochem.* **1992**, *19* (1), 133−140.
(66) Lu, S. F.; Chen, M.; Chen, C. H. Mechanisms and kinetics of thermal degradation of poly(butylene succinate-co-propylene succinate)s. *J. Appl. Polym. Sci.* **2012**, *123* (6), 3610−3619.
(67) Stein, S. E. *NIST Standard Reference Database Number 69-Infrared Spectra*; National Institute of Standards and Technology, 2018.
(68) Ma, Z.; Wang, J.; Yang, Y.; Zhang, Y.; Zhao, C.; Yu, Y.; Wang, S. Comparison of the thermal degradation behaviors and kinetics of palm oil waste under nitrogen and air atmosphere in TGA-FTIR with a complementary use of model-free and model-fitting approaches. *J. Anal. Appl. Pyrolysis* **2018**, *134*, 12−24.
(69) Hautman, D. J.; Dryer, F. L.; Schug, K. P.; Glassman, I. A Multiple-step Overall Kinetic Mechanism for the Oxidation of Hydrocarbons. *Combust. Sci. Technol.* **1981**, *25* (5−6), 219−235.
(70) Ma, Z.; Chen, D.; Gu, J.; Bao, B.; Zhang, Q. Determination of pyrolysis characteristics and kinetics of palm kernel shell using TGA-FTIR and model-free integral methods. *Energy Convers. Manage.* **2015**, *89*, 251−259.
(71) Lazdovica, K.; Liepina, L.; Kampars, V. Catalytic pyrolysis of wheat bran for hydrocarbons production in the presence of zeolites and noble-metals by using TGA-FTIR method. *Bioresour. Technol.* **2016**, *207*, 126−133.
(72) Morley, J. O.; Roberts, D. W. Molecular Modeling Studies on Aromatic Sulfonation. 1. Intermediates Formed in the Sulfonation of Toluene. *J. Org. Chem.* **1997**, *62* (21), 7358−7363.
(73) Gao, N.; Li, A.; Quan, C.; Du, L.; Duan, Y. TG-FTIR and Py-GC/MS analysis on pyrolysis and combustion of pine sawdust. *J. Anal. Appl. Pyrolysis* **2013**, *100*, 26−32.
(74) Manahan, S. E. *Toxicological Chemistry*; Lewis Publishers:, 1992.

DOI: 10.1021/acs.iecr.9b00797
Ind. Eng. Chem. Res. 2019, 58, 8112−8122